

Supporting Information

N/P-dual-doped carbon coated $\text{Na}_3\text{V}_2(\text{PO}_4)_2\text{O}_2\text{F}$ microspheres as high-performance cathode material for sodium-ion batteries

Lu-Lu Zhang¹, Jing Liu¹, Cheng Wei¹, Pan-Pan Sun¹, Lin Gao¹, Xiao-Kai Ding², Gan Liang³, Xue-Lin Yang^{1,*}, and Yun-Hui Huang^{4,*}

¹ College of Materials and Chemical Engineering, Hubei Provincial Collaborative Innovation Center for New Energy Microgrid, China Three Gorges University, 8 Daxue Road, Yichang, Hubei 443002, China

² School of Chemical Engineering & Light Industry, Guangdong University of Technology, Guangzhou, 510006, Guangdong, China

³ Department of Physics, Sam Houston State University, Huntsville, Texas 77341, USA

⁴ School of Materials Science and Engineering, State Key Laboratory of Material Processing and Die & Mould Technology, Huazhong University of Science and Technology, 1037 Luoyu Road, Wuhan, Hubei 430074, China

*Corresponding authors: xlyang@ctgu.edu.cn; huangyh@hust.edu.cn

Material characterization

The crystal structure and phase of the obtained samples were examined by X-ray powder diffraction (XRD, Rigaku RINT-2000) with Cu-K α radiation, and the diffraction data was recorded within the 2 θ range from 10 to 80°. The structural refinement was carried out by the Rietveld method using the GSAS software. The morphology was observed by a field emission scanning electron microscopy (FESEM, JSM-7500F, JEOL) and a high resolution transmission electron microscope (HRTEM, Talos F200X, Thermo Fisher). To verify whether nitrogen and phosphorus are doped into the carbon coating on the NVPOF@P/N/C surface, X-ray photoelectron spectroscopy (XPS, PHI Quantera, U-P) was conducted. The specific surface area and pore size distribution were analyzed by Brunauer-Emmett-Teller (BET) nitrogen adsorption-desorption measurement (ASAP2020, Micromeritics). The carbon content and electronic conductivity of samples were determined by a thermal analyzer (STA 449 F3, NETZSCH, Germany) under flowing oxygen and a powder resistivity measurement system (FT-300I, Rico, China), respectively. The tap density of samples was measured by a powder vibration densitometer (JZ-1, Chengdu Jingxin).

Electrochemical measurements

The cathode electrodes were fabricated by mixing active material such as NVPOF, NVPOF@C, NVPOF@N/C, NVPOF@P/C and NVPOF@P/N/C (80 wt.%) with acetylene black conductor (10 wt.%) and PVDF binder (10 wt.%) in N-methyl-2-pyrrolidone. The mixed slurry was uniformly pasted on an Al foil to

obtain the electrode film. After drying, the film was punched into discs (14 mm in diameter) and pressed with ~6 MPa pressure. After drying at 120 °C for 12 h in vacuum, the electrode discs were transferred into an argon-filled glove box (Super 1220/750, Mikrouna). To assemble the CR2025 coin cells, the obtained discs were used as working electrode, sodium flake as anode electrode, Grade GF/D as separators, and 1M NaClO₄/(EC+DMC+EMC) (volume ratio, 1:1:1) with 2 vol.% FEC (fluoroethylene carbonate) as electrolyte. The mass loading of electrodes is ~1.2 mg cm⁻². Galvanostatic charge/discharge measurements were performed within the voltage range of 3.0-4.5 V at room temperature on a cell testing system (CT2001A, LAND). The cyclic voltammetry (CV) tests in the voltage range between 3.0-4.5 V and electrochemical impedance spectra (EIS) measurements with the frequency range from 0.01 Hz to 100 kHz were performed on electrochemical working station (CHI614C, China).

Table S1 The R_{ct} and D_{Na^+} values from EIS data of samples.

| Samples | R_{ct} / Ω | $D_{Na^+} / \text{cm}^2 \text{ s}^{-1}$ |
|-------------|-------------------|---|
| NVPOF | 474.8 | 6.7×10^{-14} |
| NVPOF@C | 453.3 | 7.3×10^{-14} |
| NVPOF@P/C | 311.1 | 1.5×10^{-13} |
| NVPOF@N/C | 324.8 | 1.4×10^{-13} |
| NVPOF@P/N/C | 233.5 | 2.8×10^{-13} |

Table S2 The discharge capacity (D.C.) and capacity retention (C.R.) of samples.

| Samples | 0.5 C | | | 2 C | | |
|-------------|-----------------------------|-------------------|-------------------|-----------------------------|-------------------|-------------------|
| | D.C. (mAh g ⁻¹) | | C.R. ^a | D.C. (mAh g ⁻¹) | | C.R. ^b |
| | 1 st | 100 th | (%) | 1 st | 500 th | (%) |
| NVPOF | 84.2 | 69.9 | 83.0 | 51.4 | 27.0 | 52.5 |
| NVPOF@C | 116.3 | 98.5 | 84.7 | 92.1 | 55.0 | 59.7 |
| NVPOF@P/C | 120.5 | 111.3 | 92.4 | 112.1 | 89.6 | 79.9 |
| NVPOF@N/C | 117.4 | 97.7 | 83.2 | 109.8 | 75.9 | 69.1 |
| NVPOF@P/N/C | 128.0 | 118.7 | 92.7 | 122.0 | 99.4 | 81.5 |

C.R.^a is the capacity retention ratio of the 100th capacity to the 1st capacity at 0.5 C.

C.R.^b is the capacity retention ratio of the 500th capacity to the 1st capacity at 2 C.

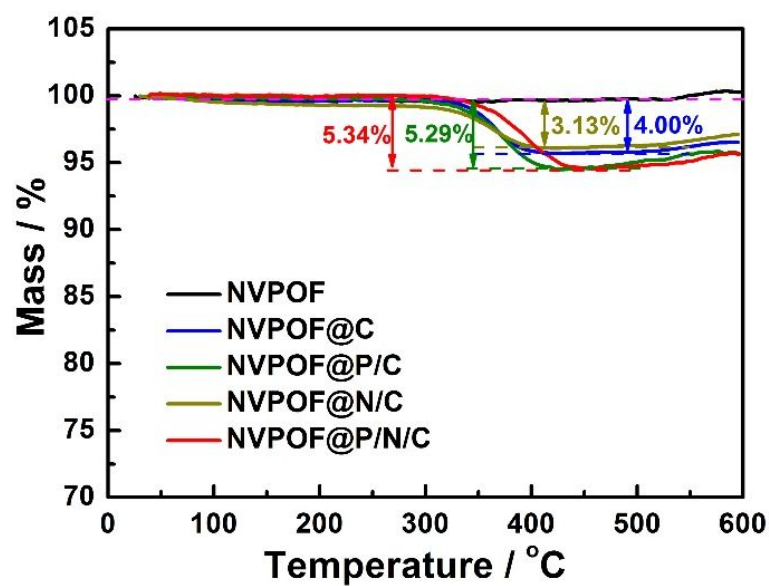


Figure S1 TG curves of NVPOF, NVPOF@C, NVPOF@P/C, NVPOF@N/C and NVPOF@P/N/C.

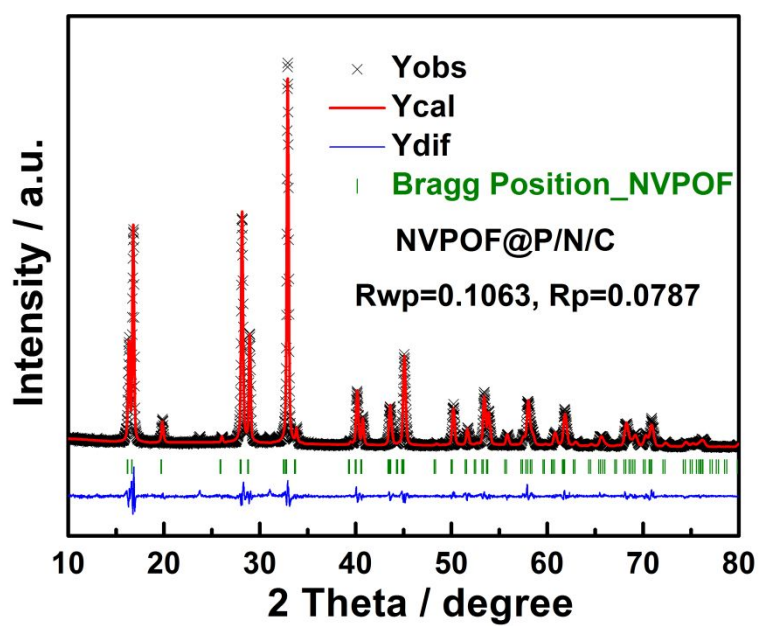


Figure S2 The Rietveld refinement results of NVPOF@P/N/C.

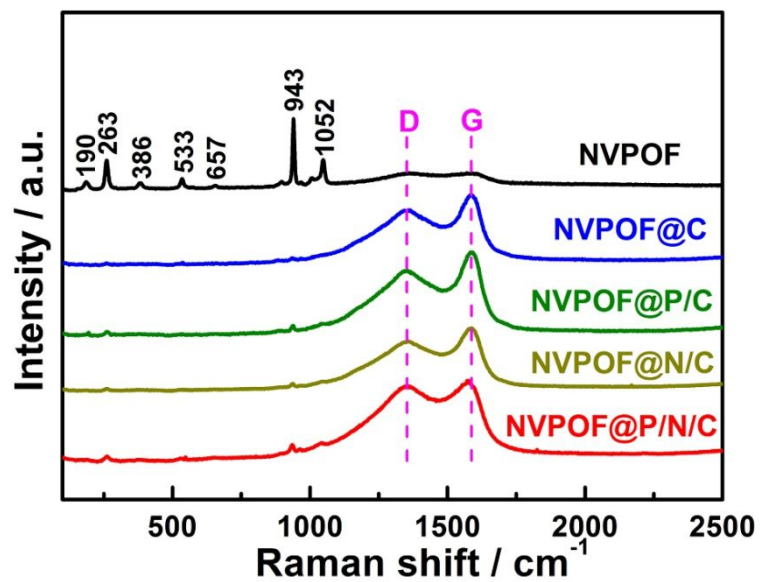


Figure S3 Raman spectra of NVPOF, NVPOF@C, NVPOF@P/C, NVPOF@N/C and NVPOF@P/N/C.

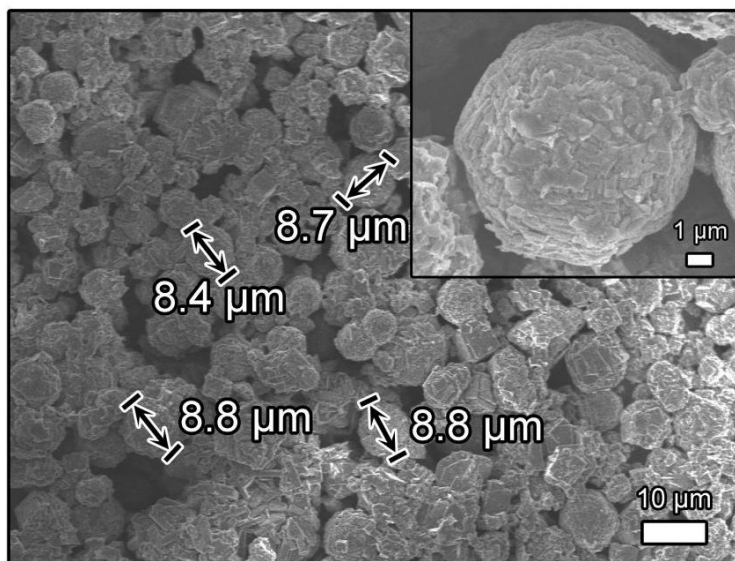


Figure S4 SEM image of the NVPOF@P/N/C precursor. The inset is the corresponding high-magnification SEM image.

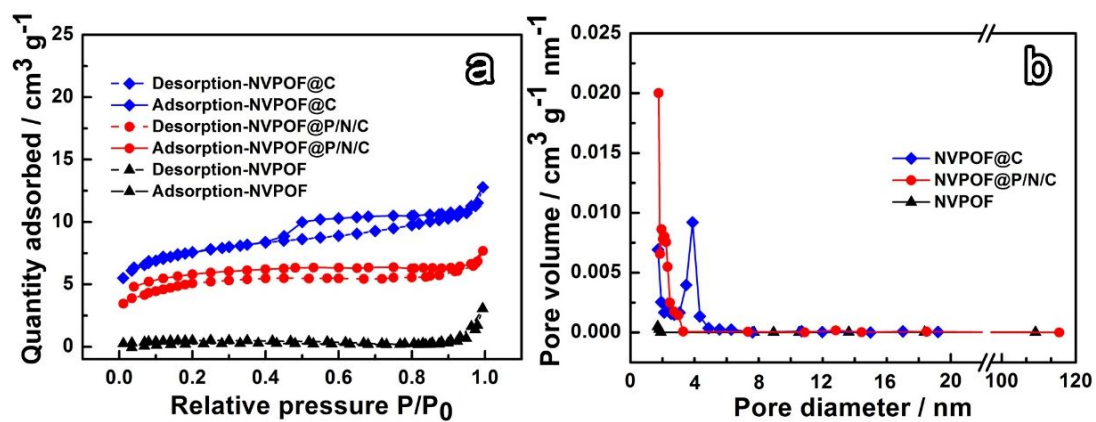


Figure S5 (a) Nitrogen adsorption-desorption isotherms, and (b) BJH pore size distribution of NVPOF, NVPOF@C and NVPOF@P/N/C.

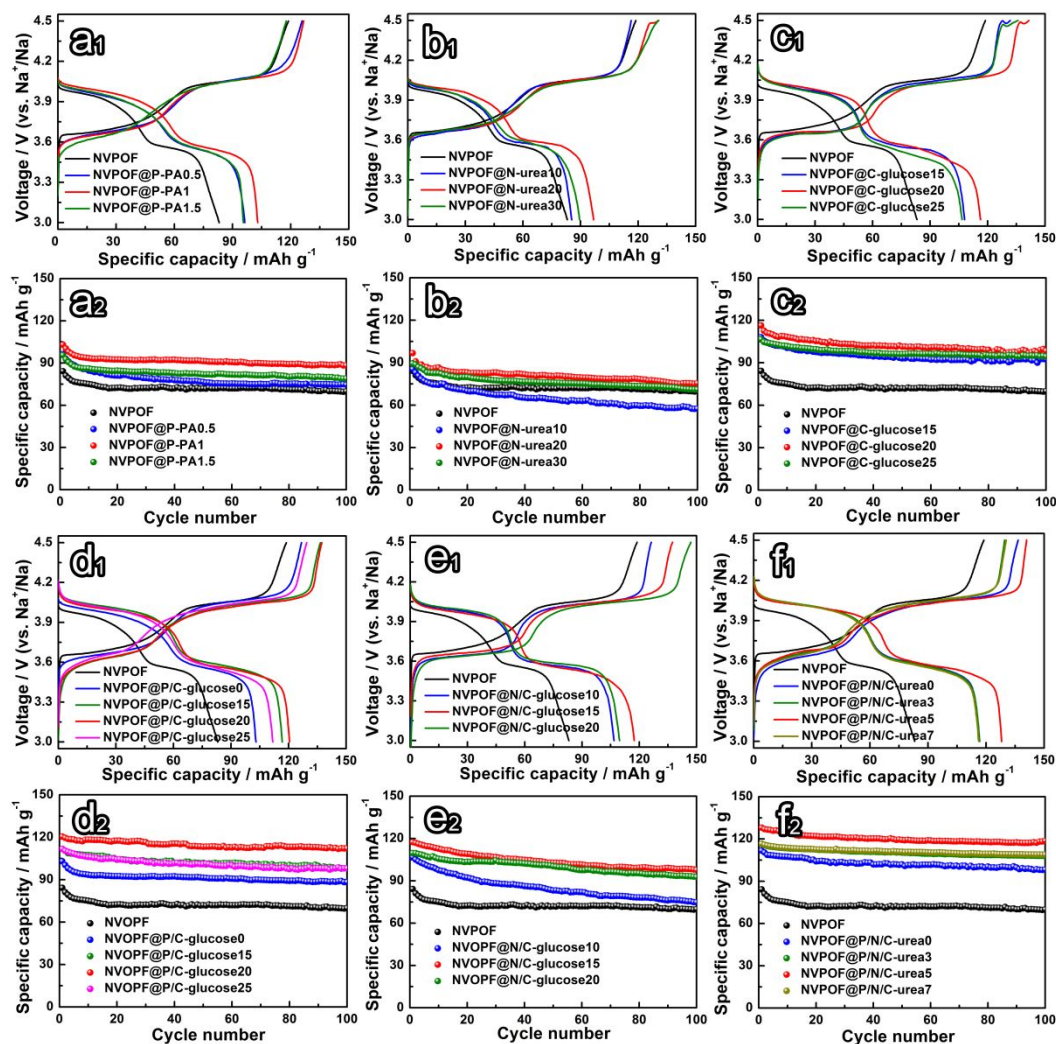


Figure S6 (a₁,a₂) Charge/discharge profiles and cycle performance of NVPOF@P with different amount of PA. (b₁,b₂) Charge/discharge profiles and cycle performance of NVPOF@N with different amount of urea. (c₁,c₂) Charge/discharge profiles and cycle performance of NVPOF@C with different amount of glucose. (d₁,d₂) Charge/discharge profiles and cycle performance of NVPOF@P/C with different amount of PA and glucose. (e₁,e₂) Charge/discharge profiles and cycle performance of NVPOF@N/C with different amount of urea and glucose. (f₁,f₂) Charge / discharge

profiles and cycle performance of NVPOF@P/N/C with different amount of PA, urea and glucose.

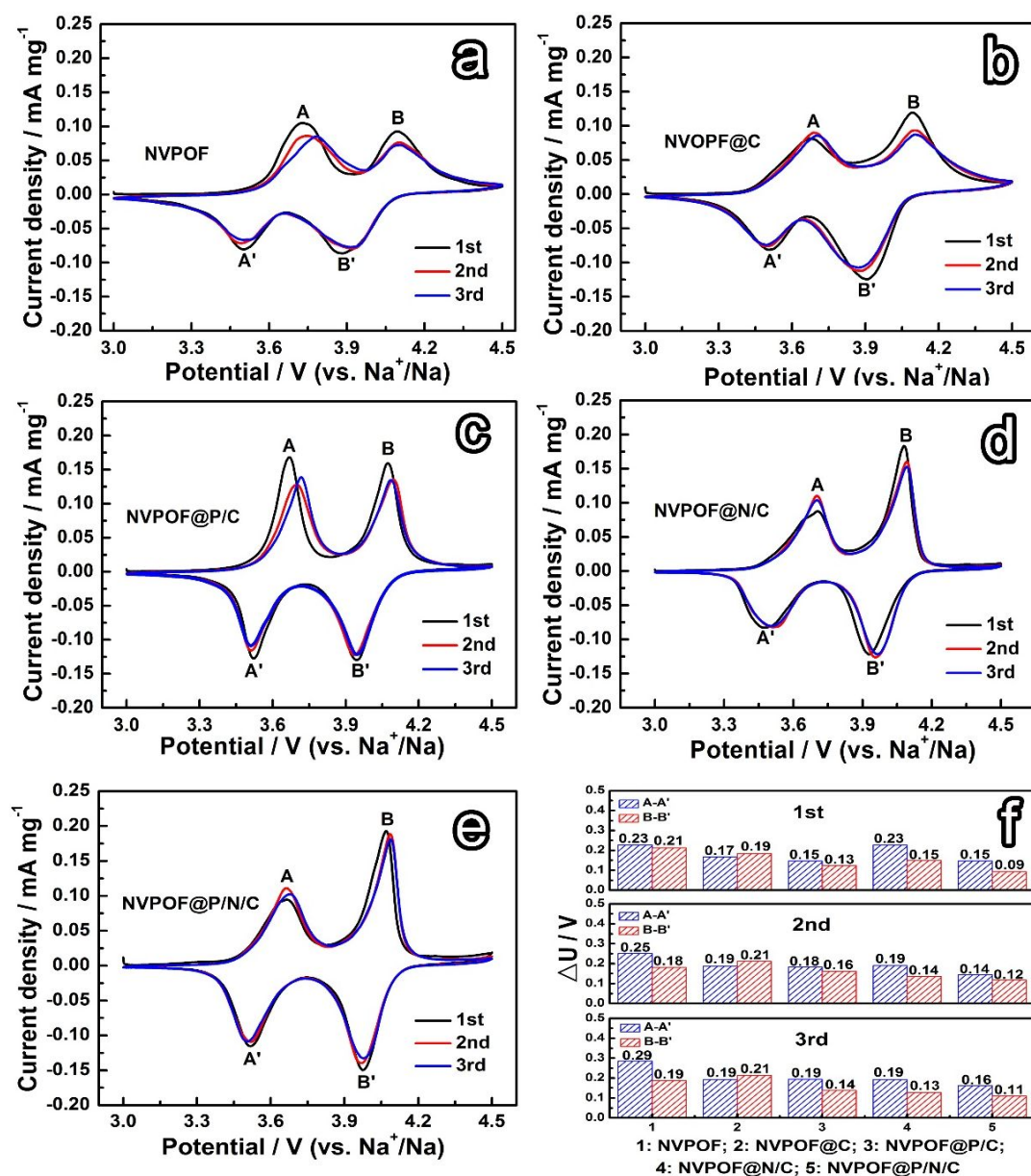


Figure S7 (a-e) CV curves of the first three cycles for the obtained samples at a scan rate of 0.1 mV s⁻¹ between 3.0 and 4.5 V. (f) The potential difference between reduction and oxidation peaks of the first three cycles for samples.

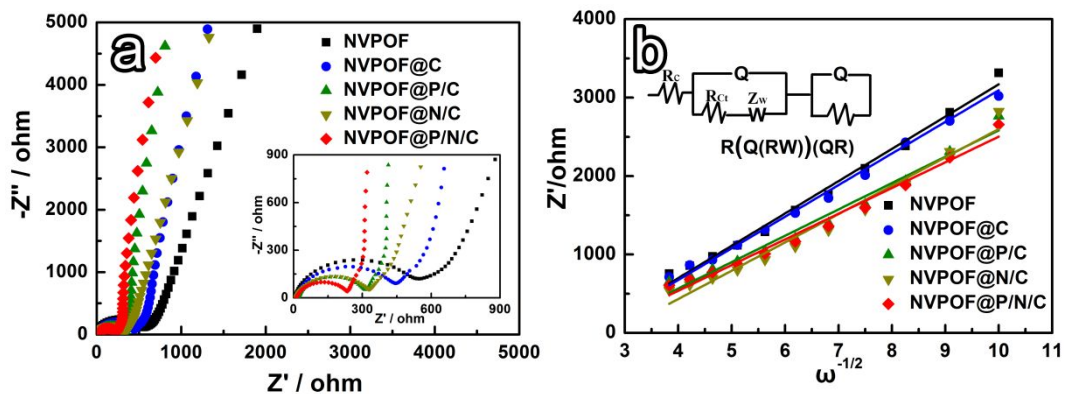


Figure S8 (a) EIS curves with the frequency range from 0.01 Hz to 100 kHz. (b) The relationship lines between Z' and $\omega^{-1/2}$ in the low frequency region of different fresh electrodes.